

## MULTIVARIATE ANALYSIS OF INFLUENCE OF HYDROGENATION AND RE-HEATING ON INTRINSIC MAGNETIZATION OF Co DOPED ZnO

R. MUKHERJI<sup>\*</sup>, V. MATHUR<sup>a</sup>, A. SAMARIYA<sup>b</sup>, M. MUKHERJI<sup>c</sup>

<sup>a</sup>The ICFAI University, Jaipur, INDIA

<sup>b</sup>S.S. Jain Subodh P.G. College, Jaipur, INDIA

<sup>c</sup>Amity University Rajasthan, Jaipur, INDIA

The study reveals the effect of hydrogenation and re-heating on magnetic properties Co doped ZnO. Magnetization measurements infer that pure ZnO is diamagnetic and turns to paramagnetic upon Co doping. The samples were post-annealed in hydrogen atmosphere at 50 and 300 K. Experimental findings confirms that on hydrogenation, the samples have achieved overlapped paramagnetic with ferromagnetic properties defeating the diamagnetic properties of ZnO. This study also depicts that the sample is finally returned to the paramagnetic state after re-heating. A multivariate approaches viz. cluster analysis is used to support the findings.

(Received October 16, 2016; Accepted December 5, 2016)

*Keywords:* Paramagnetic, Ferromagnetic, Cluster analysis

### 1. Introduction

The principle prerequisite for fabricating microelectronics devices is effective injection, transport, detection and manipulation of spin-polarized carriers in semiconductors at operational temperatures. This can be achieved by doping the semiconducting material with low concentrations of transition metals (TMs), producing the commonly known diluted magnetic semiconductors (DMS). Recently, a lot of studies have been done on DMS doped with TM such as II-VI: (Zn,Mn)Se, (Cd,Co)Se, (Hg,Fe)Te; IV-VI: (Sn,Mn)Te, (Pb,Mn)Te, (Pb,Eu)Te, etc[1-6]. However, the preparation of these semiconductors requires special care and facilities. Therefore, in order to make economical device fabrication methods, oxide semiconductor based DMS i.e. dilute magnetic oxide semiconductors (DMOS) has been frequently used for the last few years.

In point of fact, the oxide semiconductors exhibits numerous advantages such as wide band gap suitable for applications with short wavelength light, transparency and dyeability with pigments, high n-type carrier concentration, capability to be grown at low temperature even on plastic substrate, ecological safety and durability, low cost, etc[7]. Such benefits make oxide semiconductors more attractive. An ample amount of varieties of semiconductor oxides used as host nanomaterials, such as SnO<sub>2</sub>, ZnO, TiO<sub>2</sub>, and In<sub>2</sub>O<sub>3</sub>[8-14].

Among these, ZnO is one of most prevalent member of DMS group consisting bandgap of  $\sim 3.37$  eV, resistivity ( $\sim 10^{-2}$  cm), and large excitation binding energy (60 meV) [15]. It exhibits a wurtzite structure (*P63mc*) with lattice parameters  $a = 3.22485$  Å and  $c = 5.2054$  Å [16]. It is observed that with a certain appropriate doping into ZnO, a very highly conductive ( $3.7 \times 10^{-3}$  cm) specimen with good optical transparency ( $\sim 80-85$  %) and high carrier (electrons) density ( $1.7 \times 10^{20}$  cm<sup>-3</sup>) can be synthesized [17]. However, there are several reports available in the literature on optical and electrical properties of transition metal doped ZnO [18], but still it is a decent candidate for obtaining room temperature ferromagnetism properties, which are of significant prominence in low dimensional memory devices [19-22].

---

\*Corresponding author: rana.mukherji@gmail.com

The present work focuses on effect of hydrogenation and then re-heating on Co doped ZnO samples. A multivariate approaches viz. cluster analysis (CA) is used for interpretation of the data matrices which offers a support for the understanding of the findings.

## 2. Experimental details

Stoichiometric amounts of Zinc (II) oxide (purity 99.99%: Aldrich) and cobalt (III) oxide (purity 99.999%: Alfa Aesar) powders were used to prepare  $Zn_{0.94}Co_{0.06}O$  through solid state reaction method. [23]. The sample was then exposed for hydrogenation for ~5 hrs at 550 °C in a cylindrical quartz tube in a reduction furnace. X-ray diffraction (XRD) analyses of the samples were taken at 300K through PHILIPS X'PERT X-ray diffractometer equipped with  $CuK\alpha$  radiation. The scans were recorded from 20 to 90° with a step size of 0.02°. The crystal structures were refined using the Rietveld profile refinements program FULLPROF [24]. Field dependent magnetization measurements were ascertained at 300 K and 50 K using vibrating sample magnetometer (VSM).

### 2.1. Data Treatment

In this work, exploratory Hierarchical Cluster Analysis (HCA) analysis techniques is employed for obtaining relevant information about the data set. The main purpose of these techniques is to obtain possible relationships between the variables (Samples of pure ZnO, Co-doped ZnO, hydrogenised Co-doped ZnO and re-heated hydrogenised Co-doped ZnO).

Actually HCA is an excellent tool for preliminary data analysis and it is useful to analyze data sets for expected or unexpected clusters, including the presence of outliers. HCA examines the distances between the samples in a data set and this information is represented as a two-dimensional plot called dendrogram. In HCA each point forms, initially, a unique cluster and then the similarity matrix is analyzed. The most similar points are grouped forming one cluster and the process is repeated until all the points belong to a single cluster. As all the variables were autoscaled so that they could be compared to each other in the same scale. In the autoscaling, each element of the data matrix is mean centred and scaled to a variance of one [25, 26]. The computer package STATISTICA 8 has been used to carry out the analysis.

## 3. Result and Discussion

### 3.1. XRD refinement result

Figure 1 depicts the fitted XRD pattern of the pure ZnO. The crystal structure refinements were performed using the FULLPROF Program  $P6_3mc$  space group (No.186,  $Z=2$ ), in which each atom in the Wurtzite hexagonal structure residing on the 2b Wyckoff position with the Zn atoms at  $(1/3, 2/3, 0)$  and the O atoms at  $(1/3, 2/3, z)$  co-ordinates. The observed values of the unit cell parameters are as depicted in table 1. There was no impurity peaks detected that assures the purity of the ZnO compound, used for further cobalt doping. Figures 2 (a) and (b) shows the room temperature fitted XRD patterns of  $Zn_{0.94}Co_{0.06}O$  and the hydrogenated  $Zn_{0.94}Co_{0.06}O:H$  respectively. These diffractograms do not show any extra peaks. It thereby confirms that the hexagonal wurtzite structure is not disturbed by Co doping and hydrogenation except a small shift of all Bragg peaks i.e. attributed due to contraction of the unit cell volume (as observed in Table 1). This is owing to slightly smaller ionic radius of cobalt ( $Co^{2+} = 0.58 \text{ \AA}$ ) than that of zinc ( $Zn^{2+} = 0.60 \text{ \AA}$ ) [27]. This also indicates that Co ions have firmly been incorporated into the ZnO matrix at  $Zn^{2+}$  sites.

Profile refinement of the patterns of the  $Zn_{0.94}Co_{0.06}O$  and  $Zn_{0.94}Co_{0.06}O:H$  samples have been done to explore the effect of Co doping and hydrogenation on the structural properties. In the refinement process of the  $Zn_{0.94}Co_{0.06}O$ , Co occupancies were varied for the Zn and O(oxygen) sites to locate the exact site of dopant atoms. The preminent fit was observed when Co atoms occupy the Zn site with a total preference, whereas these atoms occupying the O site gave very poor fits.

All the atoms were easily distinguishable in the profile refinement owing to difference in their respective atomic scattering lengths of the constituent atoms. In the refinement process of  $\text{Zn}_{0.94}\text{Co}_{0.06}\text{O:H}$  sample ~6% oxygen deficiency is observed due to the hydrogenation of the sample.

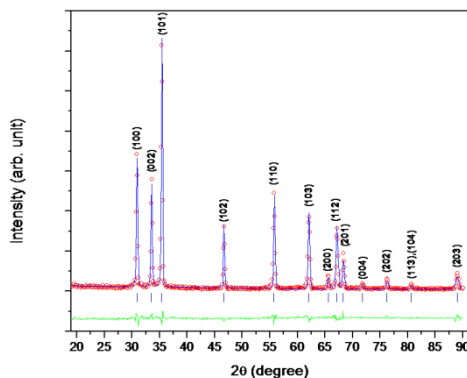


Fig. 1. Fitted and indexed XRD pattern of ZnO recorded at 300K. Observed (calculated) profiles are shown by open circle (solid line) curves. The short vertical marks represent Bragg reflections. The lower curve is the difference plot

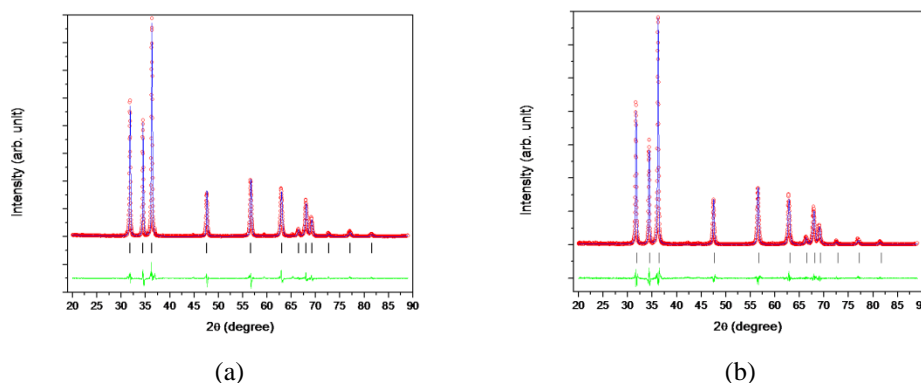


Fig. 2. Fitted XRD patterns of (a).  $\text{Zn}_{0.94}\text{Co}_{0.06}\text{O}$  recorded at 300 K and (b). Hydrogenated sample ( $\text{Zn}_{0.94}\text{Co}_{0.06}\text{O:H}$ ) recorded at 300 K. Observed (calculated) profiles are shown by open circle (solid line) curves. The short vertical marks represent Bragg reflections. The lower curve is difference plot.

Table 1: The Refined structural parameters for ZnO,  $\text{Zn}_{0.94}\text{Co}_{0.06}\text{O}$  and  $\text{Zn}_{0.94}\text{Co}_{0.06}\text{O:H}$  samples. Space Group:  $P6_{3mc}$  (No.186,  $Z=2$ )

Sample	a (Å)	c(Å)	V(Å <sup>3</sup> )	Average distance Zn-O (Å)	Positional parameter and Occupancy of Oxygen		$R_{\text{Bragg}}$	$\chi^2$
					z	N		
ZnO	3.2485(5)	5.2054(5)	47.662(7)	1.9785	0.3850(5)	1.00	3.85	1.66
$\text{Zn}_{0.94}\text{Co}_{0.06}\text{O}$	3.2433(3)	5.1944(5)	47.352(7)	1.9735	0.3781(4)	1.00	1.96	1.93
$\text{Zn}_{0.94}\text{Co}_{0.06}\text{O:H}$	3.2412(3)	5.1928(6)	47.273(8)	1.9720	0.3774(5)	0.94(1)	2.41	1.57

The results listed in table 1, confirm the single phase nature and stoichiometry of all the samples.

### 3.2. Magnetization data with multivariate analysis

The figure 3 shows the Dendrogram derived by clustering the ZnO data sets ( including pure, Co-doped and hydrogenated and then re-heated ZnO samples). The dendrogram comprises three clusters viz. are group 1 is comprised of ZnO . This group depicts a clear diamagnetic behaviour of un-doped ZnO pellet recorded at 300 K and 50K as observed in the magnetization versus applied field (M-H) curves (Figure 4) [28,29].

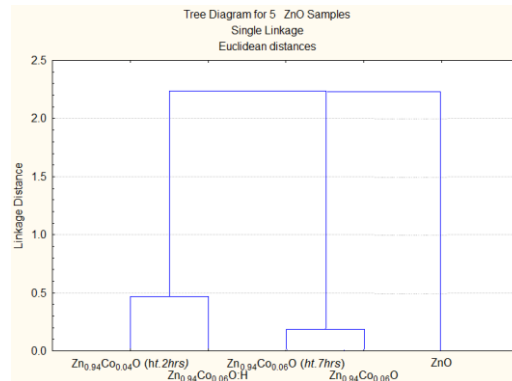


Fig. 3. Dendrogram of Hierarchical Cluster Analysis of ZnO samples

The group 2 constituting  $Zn_{0.94}Co_{0.06}O$  and reheated upto 7 hours  $Zn_{0.94}Co_{0.06}O:H$  samples. Both the samples exhibit paramagnetic behavior. Figure 5(a) show the M-H curves for the as-prepared  $Zn_{0.94}Co_{0.06}O$  recorded at 300 K. The estimated value of the effective moment using Curie's law is found to be  $0.724 \mu B/Co$ .

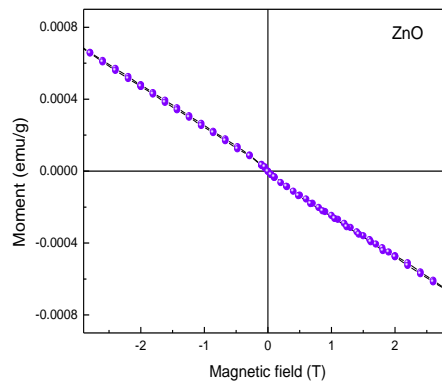


Fig. 4. M-H curve for pure ZnO measured at 300 K showing a diamagnetic state

The hydrogenated sample ( $Zn_{0.94}Co_{0.06}O:H$ ) showed a significant ferromagnetic ordering as depicted by the shape of M-H curves, the magnitudes of saturation magnetization ( $M_s$ ), the coercivity and the retentivity (Figure 5 (b)). The saturation magnetization is  $\sim 3.1$  emu/g. This is in agreement with the findings that the hydrogenation causes a robust increase in ferromagnetic ordering in Co doped samples [30-32].

Sample  $Zn_{0.94}Co_{0.06}O:H$  was then heated for nearly two hrs in air at  $550^\circ C$  which showed appreciable depression in magnetic moment (Figure 5(c)) and coercivity (both by  $\sim$  an order of magnitude) which exhibits weak FM .Therefore, in Dendrogram, both the samples are constituting group 3.

The hydrogenated sample still heated for longer duration for nearly seven hrs. The M-H curve for the heated sample (Figure 5 (d)) shows that the sample is finally returned to the paramagnetic state after long heating. Consequently, it is in group 2 of the Dendrogram. The figure 5(a) and 5(d) both are showing identical shapes.

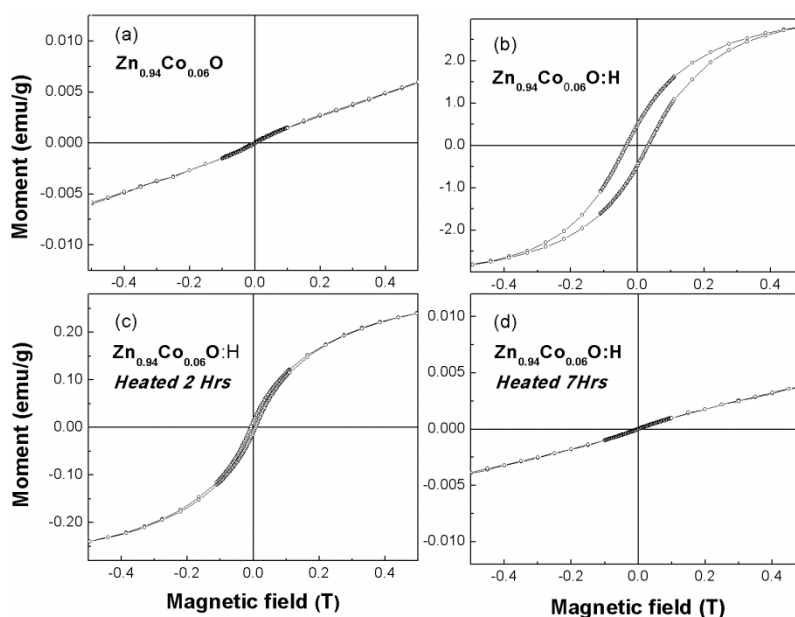


Fig. 5 M-H curves recorded at 300 K for (a). As-prepared  $Zn_{0.94}Co_{0.06}O$  (b). Hydrogenated  $Zn_{0.94}Co_{0.06}O$  (c). Heated 1 sample (2 hrs)  $Zn_{0.96}Co_{0.04}O$  and (d). Heated 2 sample (6 hrs)  $Zn_{0.94}Co_{0.06}O$ .

In order to estimate the magnitudes of the saturation magnetization, coercivity and remanence, the high field (up to 2 T) magnetization measurements were performed for the hydrogenated sample  $Zn_{0.94}Co_{0.06}O:H$  at 50 K and 300 K. Figure 6 displays well saturated ferromagnetic M-H loops of the hydrogenated sample and the obtained values of the magnetic parameters are listed in Table 2. At 50 K the remanence and coercivity show remarkable enhancement for the hydrogenated sample (coercivity shoots up from 0.041 T at 300 K to  $\sim 0.082$  T at 50 K, see Figure 6(b)).

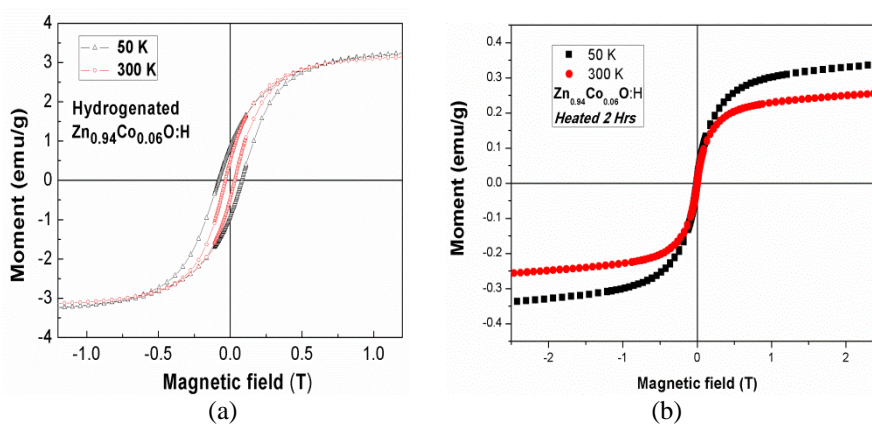


Fig. 6. Comparison of M-H curves for hydrogenated samples  $Zn_{0.94}Co_{0.06}O:H$  and heated  $Zn_{0.94}Co_{0.06}O:H$  at 300 K and 50 K.

Table 2. The magnetic moment, coercivity, retentivity and the resistance values for ZnO and Zn<sub>0.94</sub>Co<sub>0.06</sub>O sample before and after hydrogenation and after the heat treatment.

Sample	Saturation Moment (emu/g)		Coercivity (Tesla)		Remanence (emu/g)		Resistance (in Ω)
	[300 K]	[50 K]	[300 K]	[50 K]	[300 K]	[50 K]	
ZnO	Dia	Dia	-	-	-	-	100 K
Zn <sub>0.94</sub> Co <sub>0.06</sub> O	Para	Para	-	-	-	-	580 G
Zn <sub>0.94</sub> Co <sub>0.06</sub> O:H	3.1	3.22	0.041	0.082	0.486	0.884	2.2 G
Zn <sub>0.94</sub> Co <sub>0.04</sub> O (ht.2hrs)	0.254	0.336	0.036	0.022	0.05	0.06	102 G
Zn <sub>0.94</sub> Co <sub>0.06</sub> O (ht.6hrs)	Para	Para	-	-	-	-	600 G

#### 4. Conclusions

Magnetization measurements infer that pure ZnO is diamagnetic and turns to paramagnetic upon Co doping. Hydrogenation further induces a huge ferromagnetism at 300K that vanishes upon re-heating.

Experimental findings confirm the induced ferromagnetism to be intrinsic. Based on the statistical assessment, different ZnO samples are clearly divided into three groups, which are grouped as diamagnetic, paramagnetic and ferromagnetic behaviour of the pure, Co-doped, hydrogenised and then re-heated ZnO samples. Dendrogram obtained by HCA methods also support the finding of the analysis.

#### References

- [1] R. K. Singhal, A. Samariya, S. Kumarb, S. C. Sharma, Y. T. Xing, U. P. Deshpande, T. Shripathid, E. Saitovitch, J. Applied Surface Science. **257**, 1053(2010).
- [2] R. K. Singhal, A. Samariya, Y. T. Xing, S. Kumar, S. N. Dolia, T. Shripathi, U. P. Deshpande, E. Saitovitch, J. Alloys Compound. **496**, 324 (2010).
- [3] R. K. Singhal, S. Kumar, A. Samariya, M. Dhawan, S. C. Sharma, Y. T. Xing, J. Materials Chemistry and Physics **132**, 534 (2012).
- [4] S. J. Pearton, C. R. Abernathy, M. E. Overberg, J Applied Physics. **93**, 1 (2003).
- [5] X. L. Li, Q. Shifei, J. Fengxian, Q. Zhiyong, X. Xiaohong, J. Science China-Physics, Mechanics & Astronomy. **56**, 111 (2013).
- [6] O. Hideo, A window on the future of spintronics, J. Nature materials, **9**, 952 (2010).
- [7] N. Bao, Dissertation. Room Temperature Ferromagnetism Study of TiO<sub>2</sub> Based Magnetic Semiconductors By Pulsed Laser Deposition, National University of Singapore (2013).
- [8] T. Mizokawa, T. Nambu, A. Fujimori, T. Fukumura, M. Kawasaki, J. Physical Review B. doi.org/10.1103/PhysRevB.65.085209(2002).
- [9] T. Dietl, More than just room temperature., Nat. Mater. doi:10.1038/nmat2918(2010).
- [10] J. M. D. Coey, M. Venkatesan, C. B. Fitzgerald, J. Nature materials **4**,173 (2005).
- [11] Y. Matsumoto, M. Murakami, T. Shono, T. Hasegawa, T. Fukumura, M. Kawasaki, P. Ahmet, T. Chikyow, S. Koshihara, H. Koinuma, J. Science, **291**, 854 (2001).
- [12] P. Sharma, A. Gupta, K. V. Rao, F. J. Owens, R. Sharma, R. Ahuja, J. M. Osorio, B. Johansson, J. Nature materials **2**, 673, (2003).
- [13] J. J. Philip, A. Punnoose, B. I. Kim, K. M. Reddy, S. Layne, J. O. Holmes, B. Satpati, P. R. LeClair, T. S. Santos, J. S. Moodera, J. Nature Materials,

- doi: 10.1038/nmat1613 (2006).
- [14] C. Y. Hsu, Role of structural disorder in ferromagnetism of chromium-doped indium oxide J. Physics D: Applied. Physics. **44**, 415303 (2011).
- [15] A. Janotti, C.G. Van de Walle: Rep. Prog. Phys. **72**, 126501, (2009).
- [16] Powder Diffraction File, Joint Committee for Powder Diffraction Studies (JCPDS) file No. 01–080-0075.
- [17] U.Ozgu r, Y. Alivov, C. Liu, A. Teke, M. A. Reshchikov, S. Dogan, V. Avrutin, S. J. Cho, H. Morkoc, J. Appl. phys. **98**, 041301-103, (2005).
- [18] T. Dietl, J. Physics: Condensed Materials, **19**, 165204 (2007).
- [19] O.Auciello, J.F. Scott, R. Ramesh, Physics. Today, **51**, 22 (1998).
- [20] M.K.Gupta, B.Kumar, J. Material Chemistry, **21**, 14559 (2011).
- [21] S.Sharma, V.Singh, O.Parkash, R.K.Dwivedi, Applied Physics A, **112**, 975(2013).
- [22] K.N. Pham, A. Hussain, C.W.Ahn, W.Kim, S.J. Jeong, J.S. Lee, Material. Letters **64**, 2219 (2010).
- [23] R-R. Ma , F-X. Jiang, X-F. Qin, X-H Xu. Materials Chemistry and Physics, **132**, 796 (2012).
- [24] J. Rodriguez-Carvajal J 2003 FULLPROF version 3.0.0., Laboratoire Leon Brillouin, CEA- CNRS.
- [25] K. Varmuza, P. Filzmoser, Introduction to Multivariate Statistical Analysis in Chemometrics. CRC Press, Taylor & Francis Group, Boca Raton, FL (2008).
- [26] N Kumar J.I., M. Das , R. Mukherji , R. N. Kumar , J. International Environmental Application & Science, **6**(1) ,149 (2011).
- [27] S. Riaz, M. Bashir, M. A. Raza, A. Mahmood, S. IEEE Transactions on Magnetics **51**, 1 (2015).
- [28] CRC: Handbook of Chemistry and Physics, 80th edn, 1999-2000, CRC Press LLC, Boca Raton, Washington, D. C.(1999)
- [29] I. Kuryliszyn-Kudelska, W.D. Dobrowolski, L. Kilanski, B.Hadzic, N.Romcevic, D. Sibera, U.Narkiewicz, P.Dziawa, J. Phys.: Conf. Ser. **200**, 072058 (2010).
- [30] S. Jung, S. J. An, G. C. Yi, C. Jung, S.-I. Lee, and S. Cho, Applied Physics Letters **80**, 4561(2002).
- [31] P. Sharma, A. Gupta, K. V. Rao, F. J. Owens, R. Sharma, R. Ahuja, J. M. Osorio-Guillen, G. A. Gehring, Nature Materials **2**, 673 (2003).
- [32] U.Ozgu r, Y. I. Alivov, C. Liu, A. Teke, M. A. Reshchikov, S. Dogan, V. Avrutin, S. J. Cho, H. Morkoc, J. Applied Physics **98** ,041301 (2005).